Enhanced light emission from InGaN/GaN quantum wells by using surface plasmonic resonances of silver nanoparticle array*

Chen Zhan-Xu(陈湛旭)[a)b)], Wan Wei(万 巍)[a)], Zhang Bai-Jun(张佰君)[b)], He Ying-Ji(何影记)[a)], and Jin Chong-Jun(金崇君)[b)†]

[a)] School of Electronic and Information, Guangdong Polytechnic Normal University, Guangzhou 510665, China

[b)] State Key Laboratory of Optoelectronic Materials and Technologies, School of Physics and Engineering, Sun Yat-Sen University, Guangzhou 510275, China

(Received 3 June 2014; revised manuscript received 10 September 2014; published online 20 October 2014)

The effect of silver nanostructures prepared by nanosphere lithography on the photoluminescence (PL) properties of blue-emitting InGaN/GaN quantum wells (QWs) is studied. Arrays of silver nanoparticles are fabricated to yield a collective surface plasmonic resonance (SPR) near to the QWs emission wavelength. A large enhancement in peak PL intensity is observed, when the induced SPR wavelength of the nanoparticles on the QWs sample matches the QWs emission wavelength. The study proves that the SPRs could enhance the light emission efficiency of semiconductor material.

Keywords: light-emitting devices, photoluminescence, metallic nanoparticle, nanosphere lithography

PACS: 85.60.Jb, 78.55.–m, 78.67.Bf , 81.16.Nd **DOI:** 10.1088/1674-1056/23/12/128504

1. Introduction

The InGaN/GaN quantum well (QW) blue light-emitting diode (LED) has been extensively studied due to its application in white-light source, and a great improvement in light emission efficiency has been achieved. However, to compare with other white-light sources, its efficiency still needs to be further improved. So, lots of methods have been proposed to enhance the light emission efficiency. Among these methods, surface plasmon (SP) has the ability to enhance the internal and external quantum efficiency, which has attracted much attention. Basically, the SPs, including surface plasmon polariton (SPP) and localized surface plasmon (LSP), are the collective oscillations of free electrons localized at a metal/dielectric interface.[1–3] When the SP evanescent field overlaps the QW in space and spectrum, the fast energy transfer from carriers to the SPs will occur. Then, through the new emitting path, the rate of spontaneous emission would be increased.[4] Furthermore, the SPs can effectively radiate into photons and provide another emission channel when the momentum of the SP matches that of a photon. Therefore, this behavior has the potential applications in increasing the internal and external quantum efficiencies of the InGaN/GaN QW LEDs.[5–9]

In such a coupling mechanism, one of the key factors for effective light emission enhancement is the close matching between the emission wavelength and the surface plasmonic resonances (SPRs) wavelength.[10] Hence, much effort has been made to satisfy the matching condition, such as changing different kinds of metals and nanostructures.[11–20] In most cases, specific metal represents a corresponding resonance wavelength. Once a kind of metal is selected, the metal nanostructure is important to control the matching. Recently, the uses of the design and preparation of metal nanostructures to effectively couple energy between the SPRs mode and the QWs were widely reported.[10–12,16–18] For instance, the silver (Ag) nanostructures could be formed through the deposition of a thin layer of Ag followed by thermal annealing,[10,16–18] in which the dimension of nanoparticles was determined by the thickness of the Ag thin film. However, the dimensions of nanoparticles obtained are random in general. So, it is still a challenge in obtaining a well-defined metal nanostructure over a large region using economic techniques.

In this paper, we demonstrate that the use of Ag nanostructures formed by the nanosphere lithography technique on the top of an InGaN/GaN QWs can enhance the light emission. By controlling the dimensions of the nanoparticles, Ag nanoparticles can be formed and induce LSP of resonance wavelength near to the QWs emission wavelength. Then, the PL intensity becomes stronger. This method can effectively realize the energy matching between the bandgap energy of the QWs and the resonance energy of LSP. Besides, compared with conventional nanofabrication techniques, such as electron beam lithography and nanoimprint lithography, this method of nanosphere lithography can largely lower the cost.

2. Experimental methods

As shown in Fig. 1, the InGaN/GaN QWs samples were prepared to demonstrate the emission enhancement through SPRs–QWs coupling. They were grown on a 2-inch

*Project supported by the National Natural Science Foundation of China (Grant Nos. 10774195, U0834001, 10974263, 11174374, 11174061, and 10725420), the Key Program of Ministry of Education, China (Grant No. 309024), the New Century Excellent Talents in University, the National Basic Research Program of China (Grant No. 2010CB923200), and the Natural Science Foundation of Guangdong Province, China (Grant No. S2013010015795).

†Corresponding author. E-mail: jinchjun@mail.sysu.edu.cn

© 2014 Chinese Physical Society and IOP Publishing Ltd

(1 inch = 2.54 cm) sapphire substrate by metal–organic chemical vapor deposition (MOCVD). After the growth of a 3.5-μm undoped GaN buffer layer and 2.3-μm Si-doped n-GaN layer, an active layer of 3-period InGaN/GaN QWs was deposited. Then a 10-nm undoped GaN layer was deposited on the top.

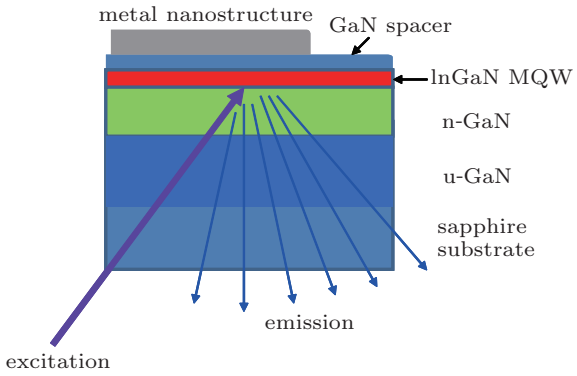


Fig. 1. (color online) Schematic illustrations of the structure of InGaN/GaN quantum wells wafer and photoluminescence (PL) measurement. The distance between the metal nanostructure layer and QWs is 10 nm. PL measurements are performed by exciting the QWs with a 405-nm laser and the incident angle is about 45°, from the back of the substrates, with collecting luminescence from backside too.

The metal nanostructures were fabricated using a nanosphere lithography technique.[21,22] The procedure can be seen from the schematic diagram in Fig. 2. Firstly, an ordered monolayer of polystyrene (PS) spheres with 450 nm in diameter was formed on the undoped GaN layer.[23,24] Secondly, in order to prepare the arrays of larger nanoparticles or nanohole arrays, the sizes of nanospheres were tailored by reactive-ion etching (RIE) with oxygen plasma, prior to deposition of the silver. The nanospheres could be etched to a smaller diameter, while maintaining the position of the sphere in the crystalline lattice. Finally, a 50-nm layer of Ag was deposited in the voids between the nanospheres using an electron beam (e-beam) evaporator. After deposition, the PS spheres were removed by sonication in trichloromethane. The formed silver monolayer nanostructures were checked by scanning electron microscopy (SEM).

For the PL measurements, the samples were pumped on a polished backside by a 405-nm diode laser, and the incident angle was about 45°. The PL was collected from the backside using an objective lens and then analyzed via a spectrometer.

Finally, we also measured the optical transmission spectra of the metal nanostructures to explain PL enhancement, which provides direct information about their plasmonic response. The transmission spectra were measured by white light illumination at normal incidence using unpolarized light. To extract the transmission features that occur due to the metal nanostructures only, all measured spectra were normalized to the transmission of the bare GaN template on sapphire.

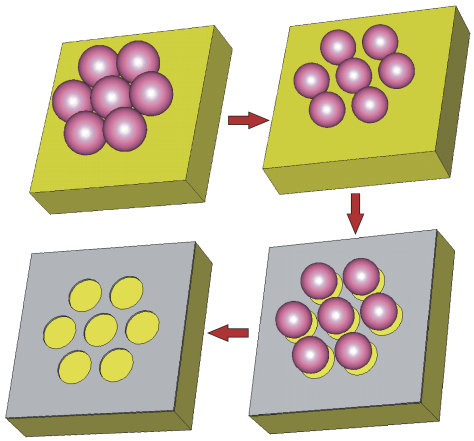


Fig. 2. (color online) Procedure for preparing Ag nanoparticles and nanoholes onto the surface of InGaN/GaN QWs.

3. Metal nanostructures

By increasing the etching time, the diameters of the nanospheres are gradually reduced, resulting in the fact that the sizes of samples with metallic nanoparticles increase to form nanohole arrays with a period identical to that of the particle array. Figure 3 shows the SEM images of the samples after removing PS spheres. When the etching time is 0 s, the nanostructure presents mostly triangle nanoparticle arrays, as shown in Fig. 3(a). With the increase of the etching time, the nanoparticles become connected in a "bow-tie" structure, as shown in Fig. 3(b). With the further increase of the etching time, the nanoparticles merge together and become a "rough" nanohole array, as shown in Fig. 3(c). When the etching time is 17 s, the metal nanostructures become an ordered nanohole array, as shown in Fig. 3(d).

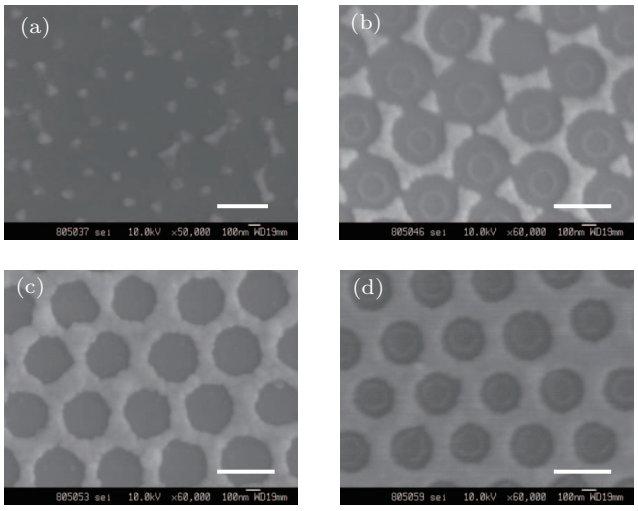


Fig. 3. SEM images of metal nanostructures onto the undoped GaN layer surfaces and the scale bars are all 400 nm. (a) The triangle nanoparticles array formed without etching the nanosphere array. (b) The connected "bow-tie" nanoparticles array formed after etching the nanosphere array for 7 s. (c) The "rough" nanohole array formed after etching the nanosphere array for 13 s. (d) The ordered nanohole array formed after etching the nanosphere array for 17 s.

4. Spectrum measurements and discussion

In Fig. 4, we compare two PL spectra measured, respectively, from an uncoated region of the QW sample and the region underneath an array of the Ag nanostructure. One can see that with the Ag nanostructures coating, the PL spectral peak is significantly enhanced and produces a blue-shifted phenomenon relative to those of the uncoated region of the QW case, and the integrated PL intensity is also significantly enhanced. The blue-shifted PL spectral peak of the coated sample could be interpreted by the quantum-confined Stark effect.[17] Figure 4 also shows the dependences of measured plasmon-enhanced luminescence on Ag nanostructures formed in different etching times. The result shows that the greatest enhancement of PL intensity can be obtained from the region coated with Ag triangle nanoparticles.

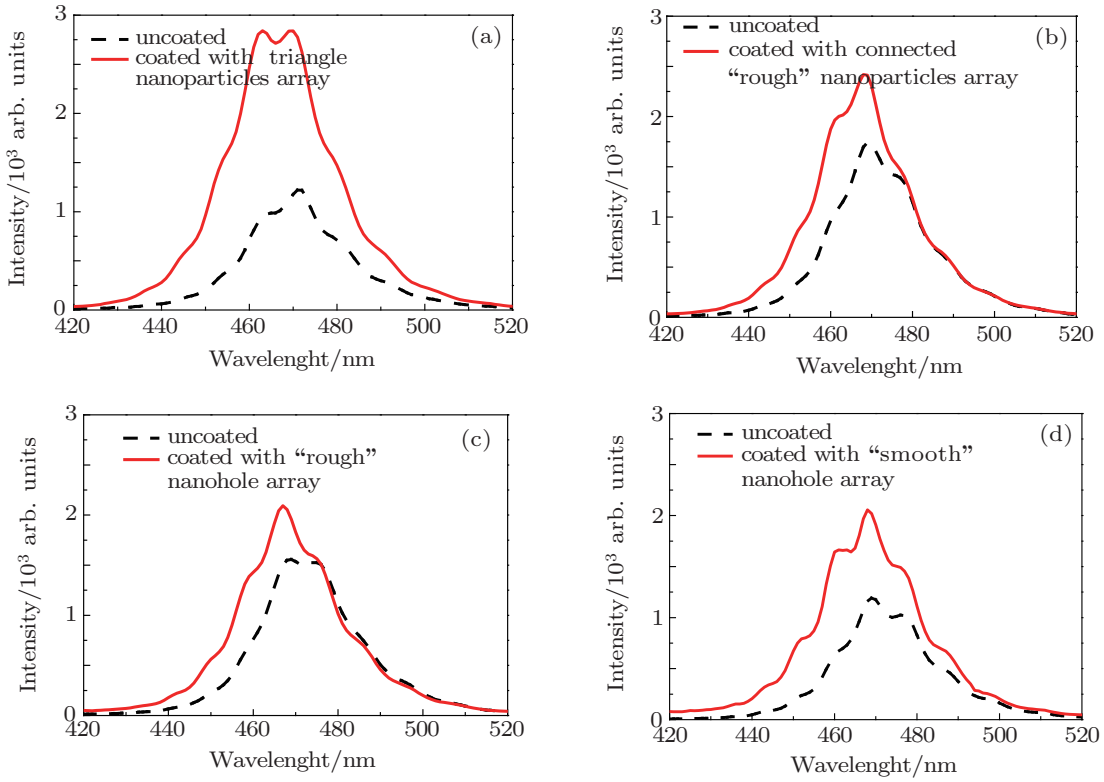


Fig. 4. (color online) (a) PL spectra measured from the region underneath the triangle nanoparticles array (solid lines) and from nearby uncoated regions (dashed lines) of the same QWs sample, (b) PL spectra measured from the region underneath the connected "bow-tie" nanoparticles array (solid lines) and from nearby uncoated regions (dashed lines) of the same QWs sample, (c) PL spectra measured from the region underneath the "rough" nanohole array (solid lines) and from nearby uncoated regions (dashed lines) of the same QWs sample, (d) PL spectra measured from the region underneath the ordered nanohole array (solid lines) and from nearby uncoated regions (dashed lines) of the same QWs sample.

In order to explain the change of plasmon-enhanced luminescence spectra, the normalized optical transmission spectra of the samples are shown in Fig. 5. There is a very clear Fabry–Pérot (FP) resonance effect, and the samples are prepared on a double-sided polished sapphire substrate. The existence of the FP resonance is due to the fact that the GaN is doped in the sapphire substrate, which can be proved by checking the oscillation period of transmission spectra. For the metallic nanostructures, the dip of transmission spectrum was associated with the main plasmonic resonance of the nanostructure.[10,11,14–18,20,25] When the etching time is 0 s, the experimental resulting structure is of Ag triangle nanoparticles mainly. The proportion of nanoparticles on the surface is small, so the transmittance is basically unchanged. This property is supported by the transmission spectrum after filtering the fast FP oscillations. However, the FP amplitude is relatively small (around 463 nm), which means that the relatively maximum absorption caused by the Ag triangle nanoparticles and the LSP resonance wavelength is around 463 nm. When the etching time is 7 s, the FP amplitude is relatively small (around 640 nm), so the absorption of the metal nanostructure should be around 640 nm. When the etching time is 13 s, the nanostructure mainly becomes a "rough" nanohole array and the FP amplitude is relatively small (around 550 nm), so the absorption of the metal nanostructure should be around 550 nm. When the etching time is 17 s, the ordered nanohole array is formed, and the FP amplitude is relatively small compared with those of the entire wavelength. In the vicinity of

416 nm, there is a dip which should be due to the bragg-surface plasmon polariton mode in the transmission spectrum of the ordered nanohole array after filtering the fast FP oscillations.[26]

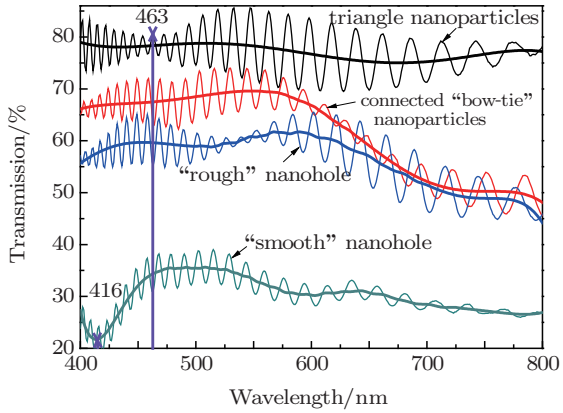


Fig. 5. (color online) Experimental optical transmission spectra of metal nanostructures. The fast oscillations are caused by the FP effect due to the existing GaN layer on the sapphire substrate. By filtering the fast FP oscillations, we can obtain the smooth curves of the transmission for the samples of triangle nanoparticles, connected "bow-tie" nanoparticles, "rough" nanohole, and ordered nanohole arrays.

The following conclusions could be derived from the results and analysis. Firstly, the enhancement of the PL does not result from the reflection of the metallic nanostructures, because the reflectivity is the minimum and the PL enhancement is highest when the QWs are coated with the Ag triangle nanoparticle array. Secondly, the PL peak wavelength is around 470 nm, and the results show that the PL will be enhanced most effectively when the resonance wavelengths of metal nanostructure are close to the emission peak wavelength. These results are in good agreement with a picture of plasmon enhanced light emission.[10,11,14–18,20,25] In this case, when the resonance wavelength of LSP is close to the QW emission wavelength, energy is transferred from the carriers in the QW to the available LSP mode via near-field electromagnetic coupling. The LSP resonance mode has zero momentum and can match the momentum of the photon, and could be effectively radiated without experiencing any other mechanism.[18,25] As a result, this represents another emission channel besides the direct dipole radiation and competes with the nonradioactive recombination processes. Furthermore, the waveguide mode in the semiconductor could also be coupled into the SP mode and effectively radiated into photons in this condition.[27,28] So this method could enhance the overall quantum efficiency of the QWs, leading to an overall increase in the measured luminescence.

For theoretical confirmation, we perform three-dimensional finite-difference time-domain simulations to calculate the transmission and reflection, and thus obtain the absorption of the samples. Figure 6 shows the simulation results of the samples covered with a Ag triangle nanoparticles array and a Ag "smooth" nanohole array, respectively. We can see that the dip (peak) wavelengths of Ag triangle nanoparticles and ordered nanoholes in simulated transmission (absorption) spectra are in good agreement with the dip wavelengths in experimental transmission spectra (after filtering the FP effect). For instance, the dip wavelengths of the Ag triangle nanoparticles array in simulation and experiment of the sample formed without etching the nanosphere array are 470 nm and 463 nm, respectively. In addition, the dips in the experiment are more broad and flat compared with the calculated results, which results from the deviation of nanoparticles in reality.

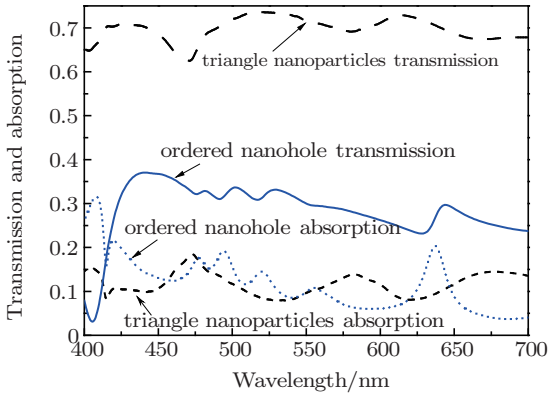


Fig. 6. (color online) Simulated transmission and absorption spectra of the Ag-triangle nanoparticle array and Ag-ordered nanohole array.

5. Conclusions

In this paper, we demonstrate SP-enhanced photoluminescence from InGaN/GaN QWs on sapphire with Ag nanostructures prepared by nanosphere lithography. The phenomena of largely enhanced PL intensity by using InGaN/GaN QWs samples with different arrays of Ag nanoparticles and nanoholes are revealed. When the resonance wavelength of the Ag nanostructures is consistent with the QWs emission wavelength, the PL of the sample will be significantly enhanced due to the matching between the QWs bandgap energy and the SPR energy. This result highlights the importance of properly designing the nanostructure for optimizing the luminescence efficiency. In addition, we find that a relatively good Ag nanostructure over a large region could be fabricated using the economic techniques of nanosphere lithography. The studies prove that the SPRs can enhance the PL efficiency of semiconductor material, and it will be a promising method for developing highly efficient solid-state light sources.

References

[1] Barnes W L, Dereux A and Ebbesen T W 2003 *Nature* **424** 824
[2] Li X P, Chen B J, Shen R S, Zhang J S, Sun J S, Cheng L H, Zhong H Y, Tian Y, Fu S B and Du G T 2013 *Chin. Phys. B* **22** 023202
[3] Wang H Y, Dou X M, Ni H Q, Niu Z C and Sun B Q 2014 *Acta Phys. Sin.* **63** 027801 (in Chinese)
[4] Okamoto K, Niki I, Shvartser A, Narukawa Y, Mukai T and Scherer A 2004 *Nat. Mater.* **3** 601

[5] Kwon M K, Kim J Y, Kim B H, Park I K, Cho C Y, Byeon C C and Park S J 2008 *Adv. Mater.* **20** 1253
[6] Cho C Y, Kim K S, Lee S J, Kwon M K, Ko H, Kim S T, Jung G Y and Park S J 2011 *Appl. Phys. Lett.* **99** 041107
[7] Cho C Y, Lee S J, Song J H, Hong S H, Lee S M, Cho Y H and Park S J 2011 *Appl. Phys. Lett.* **98** 051106
[8] Okamoto K, Niki I, Shvartser A, Maltezos G, Narukawa Y, Mukai T, Kawakami Y and Scherer A 2007 *Phys. Stat. Sol.* **204** 2103
[9] Cho C Y, KiKwon M, Lee S J, Han S H, Kang J W, EunKang S, Lee D Y and Park S J 2010 *Nanotechnology* **21** 205201
[10] Jiang S, Hu Z, Chen Z Z, Fu X X, Jiang X Z, Jiao Q Q, Yu T J and Zhang G Y 2013 *Opt. Express* **21** 12100
[11] Henson J, Dimakis E, DiMaria J, Li R, Minissale S, Negro L D, Moustakas T D and Paiella R 2010 *Opt. Express* **18** 21322
[12] Mochizuki Y, Fujii M, Hayashi S, Tsuruoka T and Akamatsu K 2009 *J. Appl. Phys.* **106** 013517
[13] Mak G Y, Fu W Y, Lam E Y and Choi H W 2009 *Phys. Status Solidi* **6** S654
[14] Sung J H, Kim B S, Choi C H, Lee M W, Lee S G, Park S G, Lee E H and O B H 2009 *Microelectron. Eng.* **86** 1120
[15] Kao C C, Su Y K, Lin C L and Chen J J 2010 *IEEE Photon. Technol. Lett.* **22** 984
[16] Oh T S, Jeong H, Lee Y S, Kim J D, Seo T H, Kim H, Park A H, Lee K J and Suh E K 2009 *Appl. Phys. Lett.* **95** 111112
[17] Yeh D M, Chen C Y, Lu Y C, Huang C F and Yang C C 2007 *Nanotechnology* **18** 265402
[18] Yeh D M, Huang C F, Chen C Y, Lu Y C and Yang C C 2008 *Nanotechnology* **19** 345201
[19] Zhao H P, Zhang J, Liu G Y and Tansu N 2011 *Appl. Phys. Lett.* **98** 151115
[20] Henson J, DiMaria J, Dimakis E, Moustakas T D and Paiella R 2012 *Opt. Lett.* **37** 79
[21] Li R, Zhu Y B, Di Y, Liu D X, Li B and Zhong W 2013 *Acta Phys. Sin.* **62** 198101 (in Chinese)
[22] Zhou Z T, Yang L, Yao J, Ye R, Xu H H and Ye Y H 2013 *Acta Phys. Sin.* **62** 188104 (in Chinese)
[23] Chen X, Liang Z H, Chen Z X, Yang W M, Chen T F, Jin C J and Zhang B J 2013 *Chin. Phys. B* **22** 048101
[24] Chen Z X, Ren Y, Xiao G H, Li J T, Chen X, Wang X H, Jin C J and Zhang B J 2014 *Chin. Phys. B* **23** 018502
[25] Huang C W, Tseng H Y, Chen C Y, Liao C H, Hsieh C, Chen K Y, Lin H Y, Chen H S, Jung Y L, Kiang Y W and Yang C C 2011 *Nanotechnology* **22** 475201
[26] Murray W A, Astilean S and Barnes W L 2004 *Phys. Rev. B* **69** 165407
[27] Sung J H, Yang J S, Kim B S, Choi C H, Lee M W, Lee S G, Park S G, Lee E H and O B H 2010 *Appl. Phys. Lett.* **96** 261105
[28] Lin C L, Chen P H, Chan C H, Lee C C, Chen C C, Chang J Y and Liu C Y 2007 *Appl. Phys. Lett.* **90** 242106